Shell features, main colonized environments, and fractal analysis of sutures in Late Jurassic ammonites

FEDERICO OLÓRIZ, PAUL PALMQVIST AND JUAN A. PÉREZ-CLAROS

LETHAIA

Olóriz, F., Palmqvist, P. & Pérez-Claros, J.A. 1997 09 15: Shell features, main colonized environments, and fractal analysis of sutures in Late Jurassic ammonites. *Lethaia*, Vol. 30, pp. 191–204. ISSN 0024-1164.

A precise approach to the quantification of relationships between suture complexity, as measured by fractal analysis (step-line procedure), the architecture of shells, and the main colonized environments, has been made in a set of Late Jurassic ammonites (N=507). Statistically significant differences between fractal-dimension (D_f) mean values of evolute and involute shells are interpreted as caused by differences in the surface:volume (S:V) ratio. Suture complexity is also related to the shape of whorl section. The lowest D_f values correspond to subcircular whorl sections (low S:V ratio) and the highest ones to acute sections (high S:V ratio). The shape of flanks shows correlation with suture complexity. The highest values of D_f are found in planulate shells and the lowest ones in whorl cross sections with convex flanks. Highly significant differences appear between D_f mean values from unsculptured shells and those from ammonites with ribs and/or tubercles of medium to large size. Multivariate analysis shows a combined variation of shell features and suture complexity, resulting in a heterogeneous distribution of D_f values within the ammonite morphospace, mainly according to structural (shell architecture) and ornamental (sculpture strength rather than density) factors. Finally, the data obtained on relationships between suture complexity and the colonized environments (epicontinental vs. epioceanic inhabitants) suggest that suture complexity is not primarily related to bathymetry, and/or that no major differences in habitat depths existed between epicontinental and epioceanic ammonites. □*Fractal analysis, factor analysis, suture lines, shell features, palaeoecology, ammonites, Upper Jurassic.*

Federico Olóriz [foloriz@goliat.ugr.es], Departamento de Estratigrafía y Paleontología, Facultad de Ciencias, Universidad de Granada, Campus de Fuentenueva, E-18002 Granada, Spain; Paul Palmqvist [Paul.Palmqvist@uma.es] and Juan A. Pérez Claros, Departamento de Ecología y Geología (Área de Paleontología), Facultad de Ciencias, Universidad de Málaga, Campus de Teatinos, E-29071 Málaga, Spain; *23rd November, 1996; revised 23rd April, 1997.*

Several approaches to the quantification of sutural complexity in ammonites and its relationship with shell geometry and/or the occupation of morphospace have been published during the last few years (Boyajian & Lutz 1992; Dommergues *et al.* 1996; Lutz & Boyajian 1995; Olóriz & Palmqvist 1995; Saunders 1995; Saunders & Swan 1984; Saunders & Work 1996; Swan & Saunders 1987).

Ammonite sutures are forms of such complexity that is not easily described by Euclidean geometry, showing very long perimeters relative to the contiguous shell areas. These sutures usually provide evidence of a 'statistical' self-similarity when observed at varying scales of magnification (i.e. the characteristic shape of the curve appears over a wide range of sizes). Accordingly, the sutures can be regarded as fractal curves (quasi-fractals *sensu* Seilacher & LaBarbera 1995) in a formal and even morphogenetic sense (Bayer 1985; Boyajian 1990, 1991; Boyajian & Lutz 1992; Damiani 1984, 1986, 1990; Checa & García-Ruíz 1996; García-Ruíz *et al.* 1990; García-Ruíz & Checa 1993; Guex 1981; Lutz & Boyajian 1995; Seilacher 1988, 1991; Slice 1993). Cranial sutures of mammalian skulls can also show high levels of complexity (although below those of ammonitic sutures), especially in stags and bovids whose skulls have to withstand stress (Long 1985; Gibert & Palmqvist 1995; Hartwig 1991).

A fractal is a shape made of parts similar in some way to the whole (Mandelbrot 1983; Sugihara & May 1990; Slice 1993). The fractal dimension (D_f) of a curve, which takes a value between one and two, may be used as a morphometric descriptor of its complexity, because a straight line has a Euclidean or topological dimension of one, and the sinuosity of a curve could closely fill a plane, thus reaching an effective or fractal dimension that approximates two.

Investigating the fractal properties of ammonite sutures, fractal analysis has been used as a morphometric tool for their precise evaluation (Boyajian & Lutz 1992; Checa & García-Ruíz 1996; García-Ruíz & Checa 1993; García-Ruiz *et al.* 1990; Lutz & Boyajian 1995; Olóriz & Palmqvist 1995; Olóriz *et al.* 1996). However, fractal analysis is weak in characterizing the differences between the three main suture types (i.e. goniatitic, ceratitic and ammonitic sutures), because suture complexity overlaps considerably between these types (Lutz & Boyajian 1995; Saunders & Work 1996). The comparatively stabilized basic structuration in sutures of ammonitic type in Late Jurassic ammonites also shows quite different sutural designs with similar folding complexity (Olóriz & Palmqvist 1995), and thus similar fractal dimensions. As a result, this morphometric procedure is inadequate for phylogenetic approaches and should be reserved for evaluating differences in the overall degree of complexity between ammonite sutures.

The measurement of suture complexity has also been approached in a different way, by using an index of suture sinuosity estimated as suture perimeter length divided by whorl circumference (Westermann 1971, 1975; Ward 1980). Sinuosity measurements (as well as fractal dimensions) do not discriminate between sutures of different geometry but with similar degree of complexity: i.e. similar values are obtained in a suture with many but shallow lobes and another with few lobes and saddles of high magnitude. Therefore, some authors have extended this approach by incorporating counts of sutural flexures (Hewitt 1985; Saunders 1995; Saunders & Work 1996). However, the sinuosity index has lower resolution for characterizing suture complexity in comparison to fractal analysis (Lutz & Boyajian 1995). As recently stated (Seilacher & LaBarbera 1995), fractal dimensions are the most elegant measurement of suture complexity. Different explanations for anticlastic septal geometry in ammonites have been proposed, including interpretations of their functional morphology (i.e. frilled sutures increased buttressing and thereby shell strength against implosion, favoured respiration and cameral liquid transport, etc.), their constructional morphology (i.e. frilled sutures resulting from body attachment, muscle attachment, mantle tie points and interactive vaulting), and physical properties (viscous fingering in fluid interfaces during morphogenesis, and compression/decompression of a bladder by fleshy membrane movability) (Bayer 1978a, b; García-Ruiz *et al.* 1990; Checa & García-Ruiuíz 1996; Hewitt & Westermann 1986, 1987; Lutz & Boyajian 1995; Olóriz & Palmqvist 1995; Pfaff 1911; Saunders 1995; Seilacher 1975, 1988; Seilacher & LaBarbera 1995; Ward & Westermann 1976; Westermann 1971, 1975, 1990).

Saunders (1995) has attempted to prove the widely accepted explanation first proposed by Buckland (1836) for sutural folding in ammonites (i.e. septal folding and fluting provided buttressing and thereby shell strength against implosion, thus allowing decreased weight in shell and septum construction), by comparing suture complexity with both shell and septum thickness in Palaeozoic ammonoids. If increased sutural complexity provided increased shell strength and thus allowed decreased weight in shell and septum construction, this should be reflected by reduced shell and/or septum thickness in forms with more complex sutures. However, Saunders (1995) found no quantitative evidence for Buckland's hypothesis. Similarly, Olóriz & Palmqvist (1995) found no support in Late Jurassic ammonites for the widespread assumption that sutural complexity, as measured by fractal analysis, is related mainly to bathymetry, as usually assumed for epicontinental *vs.* epioceanic ammonites. Ammonites that inhabited epicontinental shelves and those from swell areas of the epioceanic fringes showed similar ranges and mean values of sutural complexity.

According to Saunders (1995), two basic questions concerning ammonoid sutures remain largely unresolved: why did such different patterns in suture geometry develop independently of shell morphology, and why did these sutural patterns change so rapidly in comparison to the rather limited spectrum of shell geometries found in ammonites? In short, any relationship between suture complexity and shell geometry seems to be obscure. On the other hand, relationships between suture complexity and shell geometry have been widely accepted from early papers (Westermann 1956, 1966, 1975; Seilacher 1975) to more recent ones integrating constructional–ecological (Ward & Westermann 1985) or constructional–physiological interpretations, even considering clearly different hypotheses about the behaviour of the rear mantle (Seilacher & LaBarbera 1995; Checa & García-Ruíz 1996).

Preliminary results obtained by Olóriz & Palmqvist (1995) suggested that sutural complexity in Late Jurassic ammonites was related in a rather complex way to both shell architecture and ornamentation. The objective of this paper is to evaluate these relationships further with multivariate methods in a dataset of sutures which is larger than that used in our previous study (Olóriz & Palmqvist 1995).

Methods

The analysed sutures were compiled and photocopied from the bibliography on Late Jurassic ammonites; more than forty references were used, from Oppel (1863) to Hantzpergue (1989). The dataset comprises 507 sutures from well-preserved, mature specimens belonging to 404 nominal species (in 72 of which were analysed 2–5 sutures), and from 28 specimens referred to as undetermined species, belonging to 118 genera/subgenera, which are distributed (as indicated in parentheses) within the

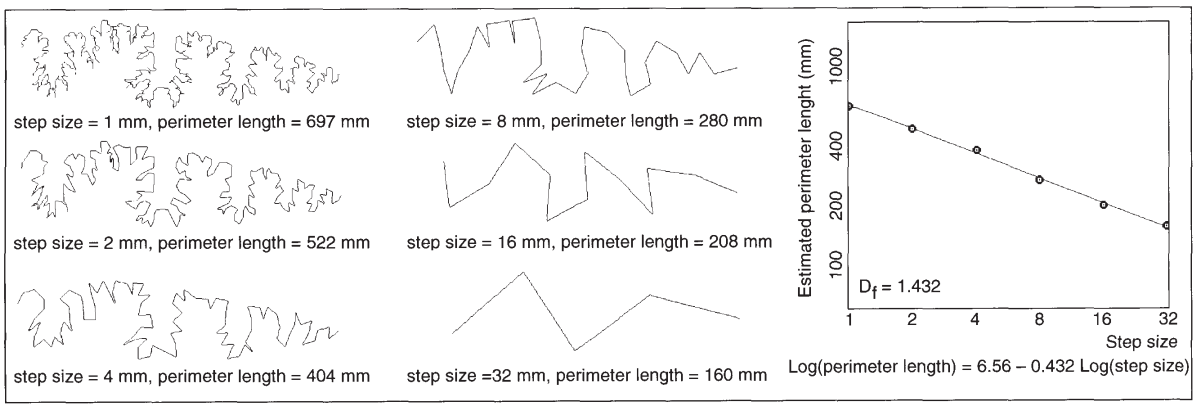

Fig. 1. Perimeter length measurement and estimation of the fractal-dimension (D_f) value of an ammonitic suture using the step-line method. The bivariate graph shows how the perimeter estimated for the curve is inversely related to the length of the ruler or step size used to measure it.

following families/subfamilies: Phylloceratina (Phylloceratidae: 12), Lytoceratina (Lytoceratidae: 2; Bochianitidae: 1), Ammonitina (Aspidoceratidae: 15; Ataxioceratidae: 25; Aulacostephanidae: 8; Berriasellidae: 4; Cardioceratidae: 1; Glochiceratidae: 3; Haploceratidae: 12; Himalayitidae: 5; Holcostephanidae: 2; Idoceratinae/Simoceratinae: 11; Oppeliidae: 4; Perisphinctidae: 12; Virgatitidae: 1). Moreover, 24 cases are of uncertain interpretation at the genus/subgenus level and are therefore not included in the distribution listed above. The results obtained in a subset of sutures (N=131) from this data base were reported by Olóriz & Palmqvist (1995).

Suture complexity of these ammonites was dealt with according to their fractal-dimension values. Shell architecture, in terms of coiling, shape of whorl section and sculpture, was approached in a semi-quantitative way. Two main colonized environments (epicontinental shelves, epioceanic fringes) have been considered, according to the provenance of the specimens studied. Ubiquity was also noted, but ubiquitous specimens were classified in two groups according to their precise provenance (epicontinental shelf or epioceanic fringe).

The fractal-dimension value of each ammonite septal suture was estimated following the Richardson step-line division method (Mandelbrot 1983; Sugihara & May 1990). Lutz & Boyajian (1995) have recently compared the two most commonly applied methods for determining the fractal dimension of ammonite sutures, the step-line divider or compass method and the box method. Richardson analysis (Boyajian & Lutz 1992; Lutz & Boyajian 1995; Olóriz & Palmqvist 1995) determines how the length of a curve is related to stride length of a divider, or length of the ruler, used to measure it. Lengths of fractal curves increase as the length of ruler or step-size decreases, and a log–log graph of the length measurement *vs.* corresponding strides will yield a straight line if the curve shows a truly fractal nature (Fig. 1). The fractal-dimension value of the curve is obtained from the following equation, which is adjusted by least-squares regression:

$$\text{Log(perimeter length)} = \text{Log}(k) + (1 - D_f)\,\text{Log(step size)}$$

where k is the Y-intercept or length measurement for unit ruler length (step-size=1). Box analysis (Checa & García-Ruíz 1996; García-Ruíz *et al.* 1990; García-Ruíz & Checa 1993) determines the length of a curve based on the number of squared boxes of a given size that are required to cover the curve. The length of fractal curves also increases exponentially as the box-size decreases.

Although both methods have been used for analysing sutural complexity in ammonoids, the step-line procedure and the box method differ in the coefficient of determination (r^2) value obtained for the least-squares regression of length measurements *vs.* step-size or box-size, respectively, as demonstrated by Lutz & Boyajian (1995). That is, this value is generally higher using the former procedure, since box data tend to scatter more around the regression line, particularly in the case of goniatitic and ceratitic sutures, thus providing less accuracy in the estimation of the fractal dimension of not highly complex ammonite sutures. Some caution is also necessary for estimating the correct D_f value of a curve using the box method, since Checa & García-Ruíz (1996) have demonstrated that small values of the measuring unit give information about the range of scale showing Euclidean behaviour, and the slope of this part of the regression line relating curve length to box-size is thus somewhat decreased, while for large box-sizes the number of filled boxes tends to oscillate periodically.

Lutz & Boyajian (1995) have shown that the suture sinuosity index (Ward 1980; Saunders 1995; Saunders & Work 1996), estimated as the ratio of external suture-

length to whorl circumference (i.e. suture perimeter of the digitized suture/Euclidean distance between the endpoints of the suture), is essentially a type of fractal index, which contains measurements at only two length scales. At higher complexities the sinuosity measure and the fractal dimension have equal powers of resolution; thus, in truly fractal curves, like most complex ammonoid sutures, both parameters provide the same information. However, the fractal dimension has greater resolving power at lower complexities, because it measures length at multiple scales in forms that are not truly fractal.

Sutures of specimens analysed in the present work were digitized from photocopied illustrations on a Calcomp digitizing tablet with a resolution of 0.1 mm. Sutures were photocopied in such a way that the Euclidean distance between the two endpoints was set to 100 mm. The D_f values of digitized ammonite sutures were calculated using the computer program Fractal-D (Slice 1989), following the procedure described by Olóriz & Palmqvist (1995), in which an initial reference point is chosen at one end of the contour of the digitized suture. Euclidean distance is also selected as the step-length, or unit of measurement. From the initial reference point, a new point on the contour is found, such that the Euclidean distance between this new point and the reference point is equal to the step-size. The new point now becomes the origin, and the process is repeated until the entire contour of the suture has been covered. For each step-length, the estimated perimeter length is the sum of these Euclidean distances, and if the distance between the last point of reference and the end of the contour exceeds half of the value of the step-size, the estimated length is increased by the next multiple of the unit of measurement that has been employed (Fig. 1, step-sizes 16 and 32 mm).

The set of step-sizes used in this study was 1, 2, 4, 8, 16 and 32 mm. These values were chosen on the condition that they remain equidistant in the x axis after logarithmic transformation; the largest step-size (32 mm) was set to approximately one-third the distance between the two endpoints of the sutures. Digitizing the same suture multiple times and measuring the fractal dimension produced little error ($\pm 0.001 D_f$).

Lutz & Boyajian (1995) have shown that the fractal relationship between log(length measurement) and log(step-size) is usually not linear in ammonite sutures over the entire range of scale lengths: the bivariate log–log plot is linear over a certain range and non-linear outside that range (i.e. the linear relationship no longer applies below a given value of step-size, and the graph of suture estimated length *vs.* step-length bends towards lower slopes), or shows several linear relationships with different slopes on different portions of the range (i.e. multifractal behaviour). The appropriateness of the range of step-sizes used in this study (1–32 mm) was estimated visually from the regression plot of log(curve length) on log(scale length) for each analysed specimen; all the sutures showed linear variation within this range.

Lutz & Boyajian (1995) have also indicated that the length estimated for a suture depends on the location of the point where the length measurement starts: it may be located at one or other of the two ends of the suture, or at some interior point (in this case the length is measured towards both endpoints). To account for this source of variability, we calculated D_f in a subset of sutures ($N=100$), starting the length measurement from both endpoints, and also from three randomly selected interior points; the differences between these estimates were very small ($\pm 0.005 D_f$) in most cases.

The sizes of the specimens studied and of their sutures were not included as variates in the analysis, because Boyajian & Lutz (1992) and Olóriz & Palmqvist (1995) noted that there is only a weak correlation between the fractal dimension of sutures and their size (i.e. estimated from whorl height or from half of whorl circumference) or the diameter of the shell at which the suture was measured.

The qualitative variates used to characterize shell architecture, sculpture, and palaeoenvironment were coded as follows (Fig. 2):

Shell geometry

Coiling: Evolute (1), intermediate coiling (2), and involute (3).

Shape of whorl section: Depressed (1), subcircular (2), oval (3), high oval (4), and acute (5).

Shape of the flanks: Convex (1), slightly convex (2), and planulated (3).

Venter width: Normal (1), and reduced (2).

Sculpture

Ribs: Absent (1), small to medium size (2), and large (3).

Tubercles: Absent (1), small to medium size (2), and large (3).

Other elements (ventral furrows, constrictions, and labial ridges): Absent (1), and present (2).

Palaeoecology

Main colonized environment: Epicontinental shelf (1), indistinct, with epicontinental record from ubiquitous individuals (2), indistinct, with epioceanic record from ubiquitous individuals (3), and epioceanic fringe (4).

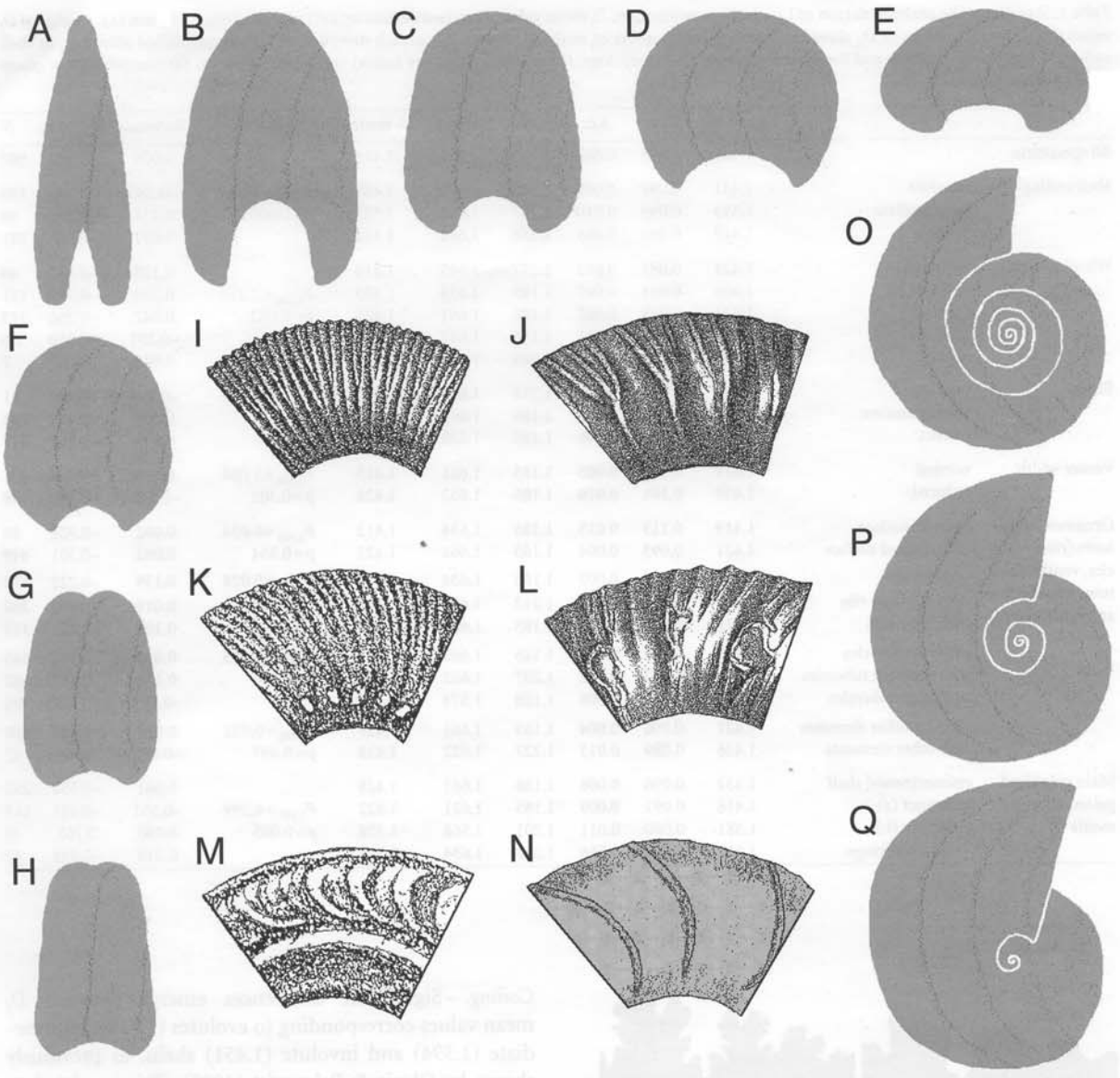

Fig. 2. Qualitative variates used to characterize shell architecture and sculpture in Late Jurassic ammonites. □Shape of whorl section: acute (a), high oval (b), oval (c), subcircular (d), and depressed (e). □Shape of flanks: convex, with venter width reduced (f), slightly convex, with venters not reduced (g), and planulated (h). □Sculpture: ribs of small to medium size (i), large ribs (j), tubercles of small to medium size (k), large tubercles (l), ventral furrow and labial ridges (m), and constrictions (n). □Shell coiling: evolute (o), intermediate coiling (p), and involute (q).

Results

Univariate analysis

The range and mean value of fractal dimensions (D_f mean=1.421, standard error of mean=0.0095, D_f min.=1.185, D_f max.=1.661) obtained for the complete set of analysed ammonite sutures (N=507; Table 1, Fig. 3) are higher than those obtained by García-Ruíz *et al.* (1990) for Mesozoic ammonites, similar to estimates deduced from Boyajian & Lutz (1992) for Late Jurassic ammonites (included in a total sample of 615 Devonian–Cretaceous ammonites), and slightly lower than estimates recently published by Olóriz & Palmqvist (1995) for a smaller dataset of Late Jurassic ammonites (N=131). When we consider different groups established according to main colonized environments, sculpture, and shell architecture, the results obtained are as follows (Table l).

Table 1. Statistics of the analysed dataset of Late Jurassic ammonites: D_f mean values, standard deviation (*s.d.*), standard error of mean (*s.e.*), range of D_f values (min., max.), median of D_f, skewness, kurtosis, and number of analysed sutures (N) in each morphologic group established according to shell coiling, shape of whorl section and flanks, sculpture, and palaeoecology. F-test values (one-way anova) and probabilities (p) for comparisons of group means are also provided.

		D_f mean	s.d.	s.e.	D_f min.	D_f max.	D_f median	Anova	Skewness	Kurtosis	N
All specimens		1.421	0.095	0.004	1.185	1.661	1.419		0.078	−0.387	507
Shell coiling	involute	1.451	0.097	0.009	1.185	1.652	1.455	$F_{2,496}=10.357$	−0.286	−0.051	120
	intermediate	1.394	0.099	0.010	1.207	1.661	1.383	$p<0.0001$	0.438	−0.216	98
	evolute	1.419	0.090	0.005	1.188	1.634	1.419		0.097	−0.361	281
Whorl section	depressed	1.424	0.083	0.012	1.277	1.595	1.419		0.128	−0.623	49
	subcircular	1.408	0.094	0.007	1.185	1.638	1.403	$F_{4,500}=2.259$	0.268	−0.282	181
	oval	1.421	0.095	0.007	1.188	1.661	1.421	$p=0.062$	0.047	−0.296	173
	high oval	1.443	0.102	0.011	1.186	1.652	1.455		−0.291	−0.310	95
	acute	1.453	0.122	0.046	1.280	1.634	1.425		0.078	−1110	7
Flanks	planulated	1.432	0.089	0.010	1.218	1.621	1.427	$F_{2,499}=2.122$	−0.177	−0.280	81
	slightly convex	1.428	0.100	0.007	1.186	1.661	1.422	$p=0.121$	0.107	−0.439	204
	convex	1.411	0.093	0.006	1.185	1.638	1.410		0.108	−0.402	217
Venter width	normal	1.419	0.094	0.005	1.185	1.661	1.415	$F_{1,505}=1.068$	0.098	−0.408	401
	reduced	1.430	0.101	0.010	1.186	1.652	1.428	$p=0.302$	−0.016	−0.340	106
Ornamental features (ribs, tubercles, ventral furrow, constrictions and labial ridges)	smooth surface	1.419	0.113	0.015	1.186	1.634	1.412	$F_{1,505}=0.034$	0.032	−0.928	58
	ornamented surface	1.421	0.093	0.004	1.185	1.661	1.421	$p=0.854$	0.092	−0.301	449
	without ribs	1.404	0.094	0.007	1.186	1.634	1.402	$F_{2,491}=5.028$	0.139	−0.222	172
	with medium ribs	1.435	0.099	0.007	1.212	1.661	1.429	$p=0.007$	0.019	−0.497	209
	with large ribs	1.419	0.091	0.009	1.185	1.622	1.419		0.102	−0.442	113
	without tubercles	1.425	0.099	0.005	1.185	1.661	1.423	$F_{2,491}=5.155$	0.057	−0.517	340
	with medium tubercles	1.436	0.097	0.012	1.207	1.652	1.426	$p=0.006$	0.138	−0.417	60
	with large tubercles	1.393	0.079	0.008	1.188	1.574	1.399		−0.222	−0.360	94
	without other elements	1.421	0.096	0.004	1.185	1.661	1.417	$F_{1,492}=0.032$	0.094	−0.423	460
	with other elements	1.426	0.089	0.013	1.227	1.622	1.428	$p=0.857$	−0.102	0.068	47
Main colonized palaeoenvironments	epicontinental shelf	1.432	0.096	0.006	1.188	1.661	1.428		0.061	−0.534	292
	indistinct (a)	1.416	0.091	0.009	1.185	1.621	1.422	$F_{3,497}=4.399$	−0.351	−0.131	113
	indistinct (b)	1.381	0.080	0.011	1.201	1.568	1.378	$p=0.005$	0.090	0.103	49
	epioceanic fringe	1.412	0.108	0.016	1.212	1.634	1.378		0.510	−0.598	47

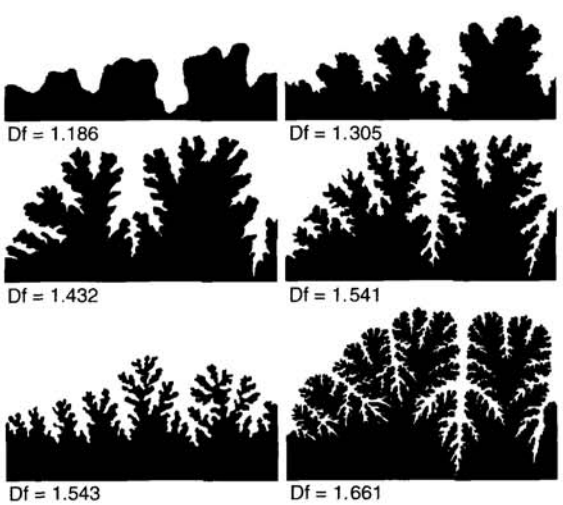

Fig. 3. Selected sutures of Late Jurassic ammonites showing different degree of complexity (folding) and their corresponding fractal-dimension (D_f) values.

Coiling. – Significant differences emerge between D_f mean values corresponding to evolutes (1.419), intermediate (1.394) and involute (1.451) shells, as previously shown by Olóriz & Palmqvist (1995). This is related to the fact that involute ammonites have camerae with a greater surface:volume (*S:V*) ratio, thus requiring strengthening. The recorded differences are statistically significant ($p<0.0001$), according to an F-test, although there is considerable overlap in the range of D_f values for these groups (Fig. 4).

Whorl section. – Significant differences are also recovered for D_f mean values of five groups of ammonites classified according to the shape of whorl section. These differences agree well with their constructional design, but their significance is hidden to a large extent behind the wide variability in D_f values found within the groups (Fig. 4). Suture lines in subcircular whorl sections show the lowest values (D_f mean=1.408), because they have low *S:V* ratios; next higher values are from suture lines in

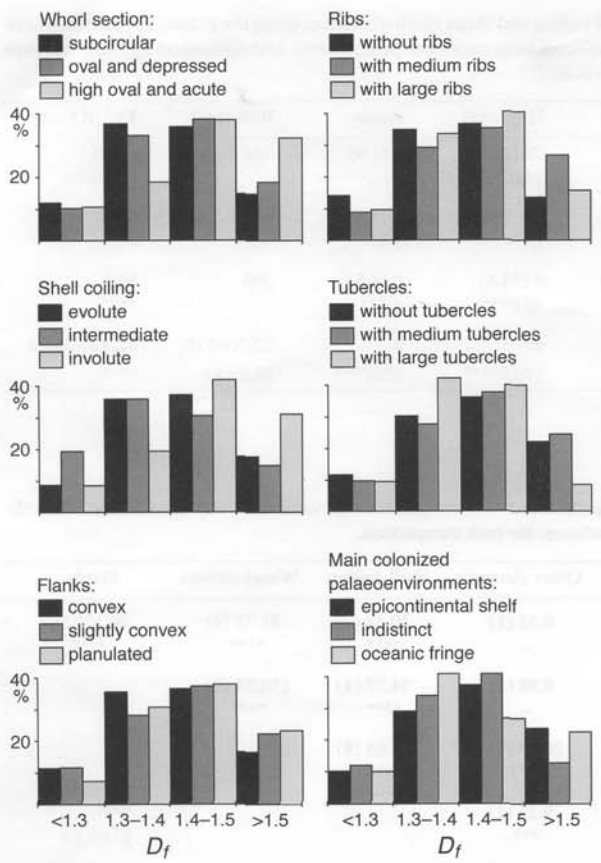

Fig. 4. Bar chart histograms for the distribution of types of whorl sections and flanks, types of shell coiling, ornamental features (ribs, tubercles), and main colonized environments in the range of D_f values.

depressed and oval whorl sections (1.424 and 1.421, respectively), which show similar *S:V* ratios; and the highest values are found in shells with high oval (1.443) and acute (1.453) sections, given that they are more compressed and thus show higher *S:V* ratios. These differences are slightly significant ($p=0.062$) when the five groups are all compared simultaneously. However, high statistical significance is obtained when extreme mean values are compared using a *t*-test (i.e. subcircular *vs.* high oval sections, $t=31.48$, $p<0.0001$). A relationship appears to exist between the type of flanks and suture complexity. The highest value of D_f mean (1.432) is found in suture lines from planulate shells and the lowest one in those from whorl sections with convex flanks (1.411). The *t*-test reveals the statistical significance of the differences between these values ($t=20.82$, $p<0.0001$). Extremely reduced venters (D_f mean=1.430) did not seem to influence suture complexity, compared with shells showing venters of 'normal' width (1.419) ($p=0.302$).

Sculpture. – Ammonite shells classified according to the type and degree of ornamentation (ribs, tubercles, furrows, constrictions and labial ridges; unsculptured specimens were considered as a separate group) show a rather complex pattern of sutural complexity, as measured by D_f values. Highly significant differences ($p=0.007$) appear between D_f mean values from unribbed shells (1.404) and those from ammonites with ribs of medium (1.435) to large (1.419) size. Non-tuberculated shells and ammonites with tubercles of medium size show more complex sutures (1.425 and 1.436, respectively) than those with coarse tubercles (1.393) ($p=0.006$). However, these differences in mean values are hidden again behind the large overlap between the range of D_f values for the analysed groups (Fig. 4). Other sculptural elements did not affect the complexity of suture lines according to statistically non-significant differences ($p=0.857$) between D_f mean values (1.421 *vs.* 1.426).

Palaeoecology. – Assumed palaeoenvironments are also related to the complexity of suture lines. Epioceanic ammonites showed a lower D_f mean value (1.412) than that obtained for epicontinental ones (1.432) ($p=0.005$), although the histograms for both D_f distributions show a considerable overlap (Fig. 4). This difference in mean values suggests that suture complexity is not easily related to bathymetry or that there were no major differences in habitat depths for epicontinental and epioceanic ammonites as recorded from swell areas.

The results obtained in the univariate comparisons reveal several substantial differences in suture design complexity, as measured by the fractal dimension of the analysed sutures. The most important difference is related to shell coiling, the shape of whorl section, the presence of ribs and tubercles, and the major environment colonized. Since there are complex relationships between selected variates, the values obtained for suture complexity should be affected in a rather intricate way. Thus, a given sculptural feature could be particularly abundant in shells that show a given shape of whorl section, and both traits of shell morphology could then reinforce or compensate each other for their respective effects on sutural complexity. To evaluate this possibility, contingency tables for comparisons between each pair of shell and environmental variates were performed, using the χ^2 test. Table 2 shows the results obtained in the analysis of the distribution of specimens according to shell coiling and whorl shape. Each cell of the contingency table shows the number of individuals that present a given combination of both shell variates (for example, the value 3 on the upper left column is the number of involutes with depressed section). In parentheses is the number of specimens that should be found if these variates were not interrelated, the individuals being randomly distributed, as an exclusive function of the abundance of both character states in the analysed dataset (in this case, 12.6 for depressed involutes). The difference between the

Table 2. Contingency table for comparisons between each different type of shell coiling and shape of whorl section, using the χ^2 test. The cells show raw or observed frequencies for each pair of coiling and whorl-section states, expected frequencies (in parentheses), and differences (χ^2-test) between observed and expected frequencies (*: $p<0.1$, **: $p<0.05$, ***: $p<0.01$, ****: $p<0.001$).

Coiling\Whorl section	Depressed	Subcircular	Oval	High oval	Acute	Row totals	$\Sigma\chi^2$ (d.f.=4)
Involutes	3 (12.6) 7.3***	11 (43.8) 24.6****	26 (42.3) 6.3**	76 (23.4) 118.2****	8 (1.9) 19.6****	124	176.0 ****
Intermediate	7 (10.0) 0.9 –	37 (34.9) 0.1 –	42 (33.8) 2.0 –	13 (18.7) 1.7 –	0 (1.5) 1.5 –	99	6.2 –
Evolutes	42 (29.4) 5.4**	133 (102.3) 9.2***	107 (98.9) 0.7 –	8 (54.8) 40.0****	0 (4.5) 4.5**	290	59.8 ****
Column totals	52	181	175	97	8	$\Sigma\Sigma N=513$	$\Sigma\Sigma\chi 2=242.0$
$\Sigma\chi^2$ (d.f.=2)	13.6***	33.9****	9.0**	159.9****	25.6****	(d.f.=8)	****

Table 3. Contingency table with the results obtained in all two-by-two comparisons of architectural and ecologic variates. D_f was transformed into ordinal scale. The cells include total χ^2 test values and degrees of freedom (in parentheses) for each comparison.

	D_f (range)	Palaeoecology	Tubercles	Ribs	Other elements	Shell coiling	Whorl section	Flanks
Reduced vault effect	2.29 (3) –	15.04 (3) ***	11.68 (2) ***	19.58 (2) ****	0.55 (1) –	30.27 (2) ****	81.78 (4) ****	30.11 (2) ****
Flanks	5.24 (6) –	31.60 (6) ****	21.24 (4) ****	39.32 (4) ****	0.98 (2) –	54.77 (4) ****	152.54 (8) ****	
Whorl section	20.58 (12) *	36.27 (12) ****	43.37 (8) ****	38.96 (8) ****	26.39 (4) ****	241.03 (8) ****		
Shell coiling	27.14 (6) ****	13.04 (6) **	26.73 (4) ****	28.29 (4) ****	9.23 (2) ***			Key: χ^2 (d. f.) *: $p<0.1$ **: $p<0.05$ ***: $p<0.01$ ****: $p<0.001$
Other elements	6.82 (3) *	8.48 (3) **	10.74 (2) ***	20.13 (2) ****				
Ribs	13.39 (6) **	80.09 (6) ****	118.20 (4) ****					
Tubercles	11.65 (6) *	149.99 (12) ****						
Palaeoecology	16.93 (9) **							

Table 4. Spearman's rank correlations among the architectural variates (shell geometry and ornamentation) and results of the multivariate analysis: eigenvalues and percentages of variance explained by the factors, sampling adequacy, factor loadings of the variates in the factors (weighing variates are marked with asterisks), and communalities for the variates.

	Venter width	Flanks	Whorl shape	Coiling	Ribs
Tubercles	–0.164	–0.220	–0.221	0.035	–0.429
Ribs	0.140	0.009	–0.093	–0.215	
Coiling	0.201	–0.010	0.468		
Whorl-section	0.344	0.366			
Flanks	0.084				
	Sampl. adeq.	Factor I	Factor II	Factor III	Communal.
Tubercles	0.548	–0.107	– 0.751*	–0.318	0.676
Ribs	0.494	–0.113	0.863*	–0.117	0.771
Coiling	0.521	0.793*	–0.279	–0.011	0.707
Whorl shape	0.524	0.720*	0.005	0.515*	0.784
Flanks	0.483	0.004	0.075	0.931*	0.872
Venter width	0.659	0.680*	0.373	–0.084	0.609
eigenvalues		1.885	1.535	1.000	
% var. explained		31.4%	25.6%	16.6%	

observed (3) and the expected (12.6) frequencies is then tested using the χ^2 statistic (7.3 for involutes with depressed section, $p<0.01$). Sums of χ^2 row values indicate, for a given shell coiling, the distribution of the different shapes of whorl section considered; conversely, column sums of χ^2 values show the distribution of each whorl shape among the three major types of shell coiling. The results of this analysis indicate a close association between both aspects of shell geometry (total $\chi^2=242$, $p<0.001$), since the distribution of whorl sections among involute and evolute ammonites departs, significantly, in both cases, from a random distribution – involute specimens are predominantly represented by high oval and acute whorl sections, while evolutes show comparatively more rounded, depressed and oval sections. On the contrary, shells with intermediate coiling are represented by raw frequencies of whorl sections similar to those expected from a random distribution.

Table 3 summarizes the results (total χ^2 values) obtained in all two-by-two comparisons of shell and environmental variates. The fractal dimension of sutures was also included in the analysis, after transformation from metric into ordinal scale (code 1 for $1.1\leq D_f<1.2$ values, code 2 for $1.2\leq D_f<1.3$ values, code 3 for $1.3\leq D_f<1.4$ values, etc.). The χ^2 test indicates that the distribution of variate states in the analysed dataset are in most cases strongly interrelated, suggesting a rather complex relationship of sutural complexity in ammonites, as measured by fractal analysis, with respect to shell geometry, sculpture, and environments.

Multivariate analysis

The complex relationship between sutural complexity and shell features has been studied following a multivariate approach, the method of *R*-mode factor analysis (see Reyment & Jöreskog 1993). Given that the variates used to characterize both shell structure (whorl coiling, shape of whorl section and flanks, venter width), as well as the type and degree of development of sculpture (ribs, tubercles) were coded in ordinal scale (i.e. qualitative variates), correlation values were estimated with the non-parametric Spearman's *rs* rank correlation coefficient (Table 4). Factor analysis was performed using the SYSTAT program, version 5.0, following the varimax procedure to rotate the factors.

The first three factors obtained in the analysis account for nearly 74% of the total variance from the six original variates, and their associated eigenvalues (λ) were statistically significant ($\lambda\geq1$, see Reyment 1991). The communalities obtained (proportion in which each variate is explained by the factors) ranged between 0.676 for tubercles and 0.872 for the shape of flanks. The histograms with the factor scores obtained for the analysed dataset of specimens in the three factors are shown in Fig. 5. The distribution of several selected ammonites showing different shell features has been included in each histogram, in order to facilitate the interpretation of the factors.

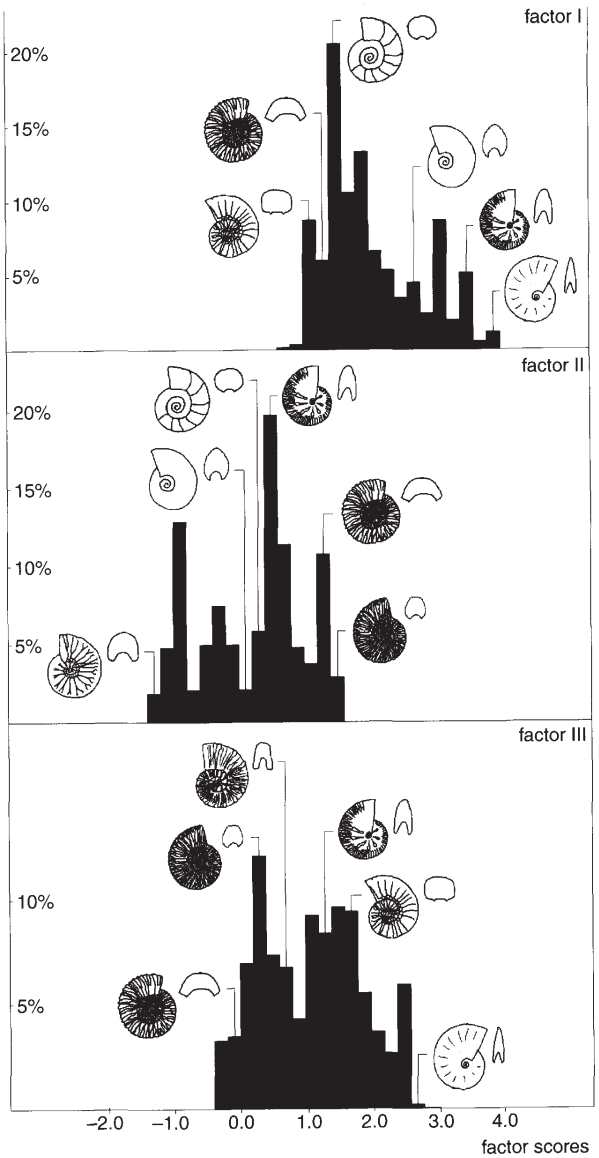

Fig. 5. Bar chart histograms for the distribution of factor score values for the analysed specimens along the three eigenvectors obtained in the factor analysis.

Inspection of the absolute magnitude and sign of factor loading coefficients for the variates in the factors (Table 4) indicated that factor *I* may be interpreted as an architectural or structural one, which distributed the analysed specimens according to coiling, the shape of whorl section and venter width, variates which all obtained high positive loadings in this vector (the remaining variates had factor loading values close to zero). Ammonite shells that were projected on the positive values of factor *I* were those

that showed involute coiling, high oval or acute whorl sections, and extremely reduced venters; specimens which received negative factor scores were evolutes, with depressed, subcircular or oval whorl sections, and with venters which were not reduced (Fig. 5).

Factor *II* is an ornamental one, which was mainly associated with shell sculpture. The only two variates that obtained high loadings in this vector were ribs and tubercles, with positive and negative signs, respectively. Ammonite shells were therefore arranged along this axis from unribbed specimens with coarse tubercles, which had negative projections, to those shells with ribs of large size and without tubercles, which received positive factor scores; unsculptured ammonites and those with weak ribs and/or tubercles were projected on intermediate values of this axis (Fig. 5).

Factor *III* indicates the type of generative curve, since it was strongly and directly correlated with both the shape of the flanks (factor loading value close to one), and to a lesser degree with the shape of whorl section. Ammonite shells were then distributed on this vector (Fig. 5) from specimens with convex flanks and rounded section (negative factor scores) to planulate shells with acute section (positive projections).

The fractal-dimension values (D_f) obtained for the specimens analysed are weakly correlated with their projections on these factors (0.111, 0.068, and –0.089 for Pearson's r correlation coefficient values between D_f and factors *I, II, a*nd *III* scores, respectively), which shows a rather complex relationship between suture complexity and shell morphology as a whole. This relationship was approached by multiple regression analysis, which showed a significant trend to increase D_f as a function of the scores obtained when the studied specimens were projected on the factors:

$$D_f = 1.382\ (\pm 0.013) + 0.014(\pm 0.006)F_I + 0.010(\pm 0.006)F_{II} + 0.008(\pm 0.006)F_{III},$$

$$r = 0.154,\ F = 3.862\ (p = 0.009),$$

where F_I, F_{II} and F_{III} are the specimen scores on factors *I*, *II* and *III*, respectively. The three partial regression slopes have positive sign, which indicates that the most complex sutures are usually found in ammonite shells with involute coiling, compressed whorl section, planulated flanks, reduced venter and large ribs; on the contrary, evolute specimens with subcircular whorl section, convex flanks, venter not reduced, unribbed and with tubercles of large size tend to show the lowest D_f values.

Figs. 6–8 show plots of ammonite shells projected on two-by-two combinations of factors *I, II* and *III* (x and y axes), where D_f is represented by contour lines (z axis) using 0.1 intervals of increasing value. These diagrams enable us to visualize the distribution of fractal-dimension measurements in the morphospace covered by

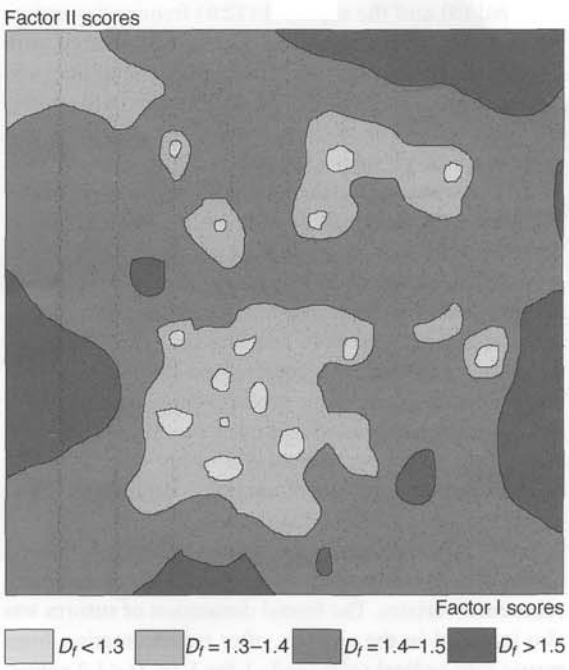

Fig. 6. Bivariate contour plot of analysed shells projected on ammonite morphospace defined by factors *I* and *II* (x and y axes, respectively). D_f is represented by contour lines (z axis) using 0.1 intervals of increasing value.

ammonite shells, as defined by factor analysis. The plot for factor *I vs.* factor *II* scores (Fig. 6) shows that specimens with complex and intricated sutures, as morphometrically characterized by high D_f values, are concentrated in four regions of the diagram: (1) positive projections on both factors (i.e. involute shells, with high oval or acute whorl sections, and prominent ribbing); (2) positive values for factor *I* and negative ones for factor *II* (i.e. involutes with high oval sections and small tubercles); (3) intermediate scores for factor *I* and negative ones for factor *II* (i.e. shells with intermediate coiling and coarse tubercles); and (4) negative values for factor *I* and intermediate ones for factor *II* (i.e. evolutes, unsculptured or with small ribs and/or tubercles). Sutures with low D_f values are concentrated mainly in a wide central region of the morphospace, which is defined by intermediate scores in both factors (i.e. shells with evolute to intermediate coiling, with depressed to subcircular whorl sections, and showing weak ribbing to smoothed shells). Thus, this plot shows the distribution of suture-line complexity according to the relationships with structural and ornamental features that were previously established using univariate statistics in the analysed ammonite dataset.

The plot for factor *I vs.* factor *III* scores (Fig. 7) shows high D_f values to be correlated mainly with high positive values in both factors (i.e. planulate involutes, with high

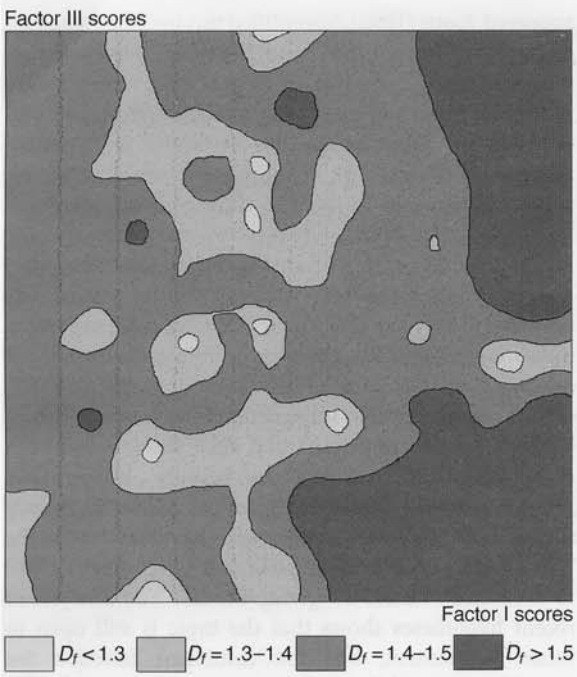

Fig. 7. Bivariate contour plot of analysed shells projected on ammonite morphospace defined by factors *I* and *III* (*x* and *y* axes, respectively). D_f is represented by contour lines (*z* axis) using 0.1 intervals of increasing value.

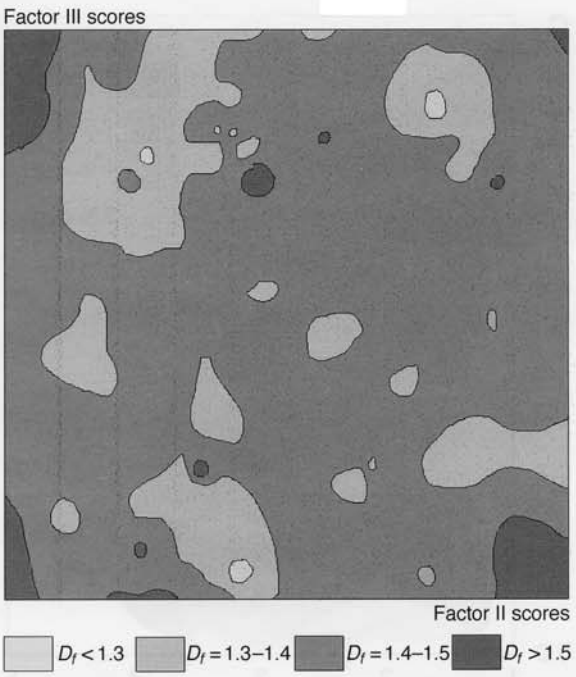

Fig. 8. Bivariate contour plot of analysed shells projected on ammonite morphospace defined by factors *II* and *III* (*x* and *y* axes, respectively). D_f is represented by contour lines (*z* axis) using 0.1 intervals of increasing value.

oval or acute sections), although intermediate to high values of D_f are also reached with negative projections on factor *III* (i.e. involute shells with convex flanks). This plot shows the distribution of suture-line complexity according to proven relationships between variates determining shell types.

The plot for factor *II vs.* factor *III* scores (Fig. 8) shows the highest values of D_f to be widely dispersed in the morphospace of the analysed ammonites, but a somewhat higher concentration of shells with complex sutures is observed on positive projections for factor *III* and negative ones for factor *II* (i.e. planulate shells with coarse tubercles), as well as for positive scores in factor *II* and negative ones in factor *III* (i.e. specimens with convex flanks and strong ribbing). Thus, this plot shows a rather intricate influence of sculpture and generative curves on suture-line complexity.

The results obtained in the multivariate analysis indicate that whorl coiling is one of the most important features determining suture complexity. Shell coiling was approached quantitatively in a subset (N=105) of the analysed specimens, using the logarithmic spiral model as defined by Raup (1967) for ammonites. Whorl expansion rate (W) and distance to coiling axis (D) were measured from accurate drawings of the shell of these specimens in axial view, obtained from the literature.

Suture complexity of the specimens, as measured by their D_f values, is directly related to W, and inversely related to D; however, the correlation values obtained in both regressions are very low and these relationships are statistically non-significant, as determined by the F-test:

$$D_f = 1.400(\pm 0.038) + 0.031(\pm 0.017)W,\ r = 0.177,\ F = 3.317\ (p = 0.071)$$

$$D_f = 1.504(\pm 0.025) - 0.098(\pm 0.067)D,\ r = 0.144,\ F = 2.146\ (p = 0.146)$$

A multiple regression approach for D_f on W and D also provided a non-significant fit (r=0.160, F=1.319, p=0.272). Fig. 9 shows the bivariate plot for the analysed specimens projected on ammonite morphospace defined by W and D, where D_f is represented by contour lines (z axis) using 0.1 intervals of increasing value. This diagram shows that both involute ($WD \leq 1$) and evolute ($WD \geq 1$) specimens with complex sutures ($D_f > 1.5$) tend to concentrate in a wide region of the morphospace which is defined by high expansion rate ($W \geq 2.5$) and low to intermediate distance to coiling axis ($D \leq 0.35$), although high values of D_f are also reached with a low expansion rate ($W \leq 2$) and a relatively high distance to coiling axis ($D \geq 0.35$).

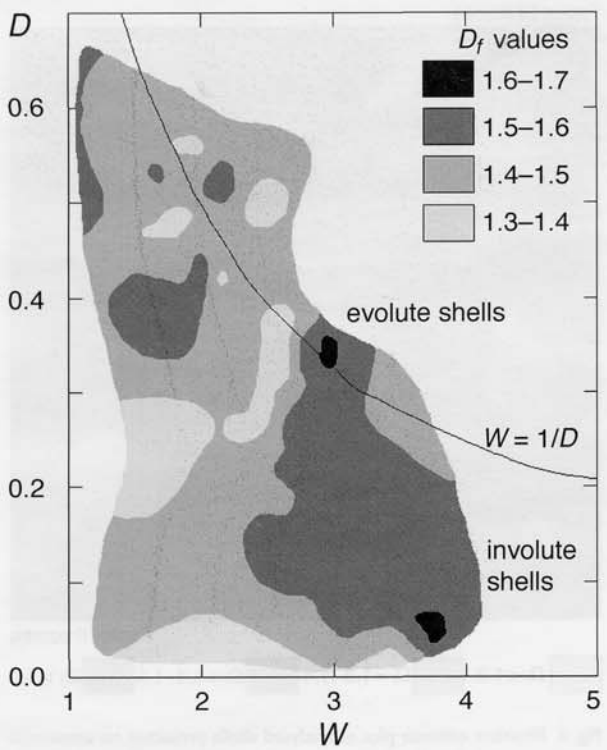

Fig. 9. Bivariate contour plot for a subset (N=105) of the analysed specimens projected on ammonite morphospace defined by whorl expansion rate (W, y axis) and distance to coiling axis (D, y axis). D_f is represented by contour lines (z axis) using 0.1 intervals of increasing value.

All the above approaches show the possibility to quantify the rather complex, but certain, relationships between the marginal frilling of suture lines and shell features in Late Jurassic ammonites, as recently revisited by Saunders (1995) for Palaeozoic ammonoids, and as previously assumed correctly by Ward & Westermann (1985), who first contributed a general qualitative picture of the intricate covariation of these features in ammonite shells.

The data obtained do not necessarily contradict those recently provided by Saunders & Work (1996) for a smaller set (117 specimens) of clearly less elaborated sutures from mainly goniatitids and secondarily prolecanitids. As in the elegant paper by Seilacher & LaBarbera (1995), the 'suture problem' of Saunders & Work (1996) must be interpreted taking into account the evolutionary scenario and the multifunctionality of biological structures. The multiple avenues for innovations in septal corrugations during the Pennsylvanian are in accordance with the persistent increase in suture complexity, as revealed by mean fractal dimensions during the Carboniferous (Boyajian & Lutz 1992). Thus, a probable decoupling of suture frilling and shell geometry occurred when main innovations in septal corrugations (addition of tie-points, whether muscular or not) and related functions appeared. Korn (1992) exemplified this for Late Devonian clymeniids. On the other hand, the long-established pattern of intricate anticlastic folding in Jurassic ammonites should be more closely related to shell features, as presented here. These ammonites developed a myriad of attachment points for incomparably more complex sutures, favouring the control during mantle displacement (Seilacher 1988). Opposite to the trend of rising mean fractal dimension of sutures during the Carboniferous, a trend towards decreasing suture complexity occurred during the Late Jurassic (Boyajian & Lutz 1992), indicating suture frilling under conditions far from those operating during the Late Carboniferous.

The controversial interpretation of relationships between suture complexity and shell features has been repeatedly assessed during this century. Westermann (1966) approached this in terms of the *'Buckman Laws of Covariation'*, Seilacher & LaBarbera (1995) referred to the *'Cartesian Divers Model'*, and Checa & García-Ruíz (1996) to a revised *'Viscous Fingering Model'*. The analysis of recent hypotheses shows that the topic is still open to future refinement, but the combined function for strengthening and floatability in ammonites could solve the 'functional mystery' (Saunders & Work 1996) of sutural complexity in ammonoids within the constraints for morphogenesis in cephalopods, and taking into account ecology and the evolutionary scenario.

Conclusions

Fractal analysis of suture lines in Late Jurassic ammonite groups based on shell geometry, sculpture and assumed palaeoenvironments, shows that sutural complexity was significantly related to shell features and less to basic ecology.

As previously stated by Olóriz & Palmqvist (1995), differences in D_f mean values in shells with variable coiling can be related to the cameral surface:volume (S:V) ratio resulting in shell strength, despite the morphogenetic pathways followed by evolute and involute shells.

Differences in suture complexity in shells with different whorl sections agree with shell architecture and the cameral S:V ratio. Therefore, shells with rounded sections, or sections with convex flanks, show lower values in the D_f mean than do those with planulated and compressed whorl sections.

Multivariate analysis shows that shell features and suture complexity combined in a rather intricate pattern. The heterogeneous distribution of D_f values in the ammonite morphospace explored suggests that suture complexity fluctuated within a nearly closed range of D_f values in connection with two relatively independent morphological factors: sculpture and shell geometry. Morphospace regions, which are occupied by mechanically reinforced

shells (i.e. heavily sculptured evolutes with subcircular whorl section, or with convex flanks), tend to show smaller D_f values than do those occupied by ammonites with weaker shells (i.e. unsculptured planulates and involutes with high oval or acute section).

More research is necessary for a precise evaluation of the influence on suture complexity of the major environments (epicontinental shelf *vs.* swell areas in the epioceanic fringe) inhabited by ammonites, but no correlation is evident between epioceanic ecospaces and depth according to the complexity of suture lines; i.e. either suture complexity was not related primarily to bathymetry or there were no major differences in habitat depths for epicontinental and epioceanic ammonites during the Late Jurassic.

Acknowledgements. – We are grateful to Dieter Korn (University of Tübingen) and Timothy Lutz (West Chester University, Pennsylvania) for helpful comments and suggestions which improved this paper. This research was financed by *Dirección General de Investigación Científica y Técnica* projects PB94-0733 and PB94-1222-CO2-02, within the framework of the *Evolución de los Márgenes Mesozoicos de Iberia* and *Foraminíferos Planctónicos* Research Groups (codes RNM 0178 and RNM 0146, Junta de Andalucía).

References

Bayer, U. 1978a: Constructional morphology of ammonite septa. *Neues Jahrbuch für Geologie und Paläontologie, Abhandlungen 157,* 150–155.

Bayer, U. 1978b: The impossibility of inverted suture lines in ammonites. *Lethaia 11,* 307–313.

Bayer, U. 1985: Pattern recognition problems in geology and paleontology. *Lecture Notes in Earth Sciences 2.* 229 pp. Springer, Berlin.

Boyajian, G.E. 1990: The fractal dimensions of ammonite sutures and their evolutionary significance. *Geological Society of America, Abstracts with Programs 22,* 308–309.

Boyajian, G.E. 1991: The fractal dimensions of ammonite sutures through geologic time. *Geological Society of America, Abstracts with Programs 23,* 38.

Boyajian, G.E. & Lutz, T. 1992: Evolution of biological complexity and its relation to taxonomic longevity in the Ammonoidea. *Geology 20,* 983–986.

Buckland, W. 1836: *Geology and Mineralogy Considered with Reference to Natural Theology. Vols. 1 & 2.*Pickering, London.

Checa, A. & García-Ruíz, J.M. 1996: Morphogenesis of the septum in ammonoids. *In* Landman, M.H., Tanabe, K. & Davis, R.K. (eds.): *Ammonoid Paleobiology,* 253–296. Plenum Press, New York, N.Y.

Damiani, G. 1984: *Il gioco della vita.* 190 pp. Editrici Italiana Audiovisivi. Roma.

Damiani, G. 1986: Significato funzionale dell'evoluzione dei sette e delle linee di sutura dei nautiloidi e degli ammonoidi. *In* Pallini, G. (ed.): *Atti I Convengo Internationale: Fossili, Evoluzione, Ambiente,* 123–130. Pergola.

Damiani, G. 1990: Computer simulation of some ammonoid suture lines. *In* Pallini, G., Cecca, F., Cresta, S. & Santantonio, M. (eds.): *Atti II Convengo Internationale: Fossili, Evoluzione, Ambiente,* 221–228. Pergola.

Dommergues, J.L., Laurin, B. & Meister, C. 1996: Evolution of ammonoid morphospace during the Early Jurassic radiation. *Paleobiology 22,* 219–240.

García-Ruíz, J.M. & Checa, A. 1993: A model for the morphogenesis of ammonoid septal sutures. *Geobios, Mem. Spec. 15,* 157–162.

García-Ruíz, J.M., Checa, A. & Rivas, P. 1990: On the origin of ammonite sutures. *Paleobiology 16,* 349–354.

Gibert, J. & Palmqvist, P. 1995: Fractal analysis of the Orce skull sutures. *Journal of Human Evolution 28,* 561–575.

Guex, 1981: Associations virtuelles et discontinuités dans la distribution des espèces fossiles: Un example intéressant. *Bulletin de la Societé Vaudoise des Sciences Naturelles 75,* 179–197.

Hantzpergue, P. 1989: Les Ammonites Kimméridgiennes du Haut-fond d'Europe Occidentale. Biochronologie. Systématique. Evolution. Paléobiogéographie. 425 pp. *Cahiers de Paléontologie,* CNRS.

Hartwig, W.C. 1991: Fractal analysis of sagittal suture morphology. *Journal of Morphology 210,* 289–298.

Hewitt, R.A. 1985: Numerical aspects of sutural ontogeny in the Ammonitina and Lytoceratina. *Neues Jahrbuch für Geologie und Paläontologie, Abhandlungen 170,* 273–290.

Hewitt, R.A. & Westermann, G.E.G. 1986: Function of complexly fluted septa in ammonoid shells. I. Mechanical principles and functional models. *Neues Jahrbuch für Geologie und Paläontologie, Abhandlungen 172,* 47–69.

Hewitt, R.A. & Westermann, G.E.G. 1987: Function of complexly fluted septa in ammonoid shells. II. Septal evolution and conclusions. *Neues Jahrbuch für Geologie und Paläontologie, Abhandlungen 174,* 135–169.

Korn, D. 1992: Relationship between shell form, septal construction and suture line in clymeniid cephalopods (Ammonoidea; Upper Devonian). *Neues Jahrbuch für Geologie und Paläontologie, Abhandlungen 185:2,* 115–130.

Long, C.A. 1985: Intricate sutures as fractal curves. *Journal of Morphology 185,* 285–295.

Lutz, T.M. & Boyajian, G.E. 1995: Fractal geometry of ammonoid sutures. *Paleobiology 21,* 329–342.

Mandelbrot, B.B. 1983: *The Fractal Geometry of Nature.* 468 pp. Freeman, New York, N.Y.

Olóriz, F. & Palmqvist, P. 1995: Sutural complexity and bathymetry in ammonites: fact or artifact? *Lethaia 28,* 167–170.

Olóriz, F., Palmqvist, P. & Pérez-Claros, J.A. 1996: Approaching the quantification of relationships between suture complexity and other shell features in Upper Jurassic ammonites. *IV International Symposium on Cephalopods – Present and Past (Granada, Spain), Abstracts* 131–133.

Oppel, A. 1863: Über jurassische Cephalopoden. *Palaeontologische Mittheilungen aus dem Museum des Koeniglich Bayerischen Staates, Stuttgart,* 127–266.

Pfaff, E. 1911: Über Form und Bau der Ammonitensepten und ihre Beziehungen zur Suturlinie. *Jahresbericht des niedersächsischen geologischen Vereins 4,* 207–223.

Raup, D.M. 1967: Geometric analysis of shell coiling: coiling in ammonoids. *Journal of Paleontology 41,* 43–65.

Reyment, R.A. 1991: *Multidimensional Palaeobiology.* 377 pp. Pergamon, Oxford.

Reyment, R.A. & Jöreskog, K.G. 1993: *Applied Factor Analysis in the Natural Sciences.* 371 pp. Cambridge University Press, Cambridge.

Saunders, W.B. 1995: The ammonoid suture problem: relationships between shell and septum thickness and suture complexity in Paleozoic ammonoids. *Paleobiology 21,* 343–355.

Saunders, W.B. & Swan, A.R.H. 1984: Morphology and morphologic diversity of mid-Carboniferous (Namurian) ammonoids in time and space. *Paleobiology 10,* 195–228.

Saunders, W.B. & Work, D.M. 1996: Shell morphology and suture complexity in Upper Carboniferous ammonoids. *Paleobiology 22,* 189–218.

Seilacher, A. 1975: Mechanische Simulation und funktionelle Evolution des Ammoniten-Septums. *Paläontologische Zeitschrift 49,* 268–286.

Seilacher, A. 1988: Why are nautiloid and ammonite sutures so different? *Neues Jahrbuch für Geologie und Paläontologie, Abhandlungen 177,* 41–69.

Seilacher, A. 1991: Self-organizing mechanisms in morphogenesis and evolution. *In* Schmidt-Kittler, N. & Vogel, K. (eds.): *Constructional Morphology and Evolution,* 251–272. Springer, Berlin.

Seilacher, A. & LaBarbera, M. 1995: Ammonites as cartesian divers. *Palaios 10,* 493–506.

Slice, D.E. 1989: *Fractal-D.* 55 pp. Exeter, New York, N.Y.

Slice, D.E. 1993: The fractal analysis of shape. *In* Marcus, L.F., Bello, E. & GarcíaValdecasas, A. (eds.): *Contributions to Morphometrics,* 161–190. Museo Nacional de Ciencias Naturales, Madrid.

Sugihara, G. & May, R. 1990: Applications of fractals in ecology. *Trends in Ecology and Evolution 5,* 79–86.

Swan, A.R.H. & Saunders, W.B. 1987: Function and shape in late Paleozoic (mid-Carboniferous) ammonoids. *Paleobiology 13,* 297–311.

Ward, P.D. 1980: Comparative shell shape distribution in Jurassic–Cretaceous ammonites and Jurassic–Tertiary nautilids. *Paleobiology 6,* 32–43.

Ward, P.D. & Westermann, G.E.G. 1985: Cephalopod paleoecology. *In* Broadhead, T.W. (ed.) *Mollusks, Notes for a Short Course,* 215–229. *University of Tennessee, Department of Geological Sciences. Studies in Geology 131.*

Westermann, G.E.G. 1956: Phylogenie der Stephanocerataceae und Perisphinctaceae des Dogger. *Neues Jahrbuch für Geologie und Paläontologie, Abhandlungen 103,* 233–279.

Westermann, G.E.G. 1966: Covariation and taxonomy of the Jurassic ammonite *Sonninia adrica* (Waagen). *Neues Jahrbuch für Geologie und Paläontologie, Abhandlungen 24,* 389–412.

Westermann, G.E.G. 1971: Form, structure and function of shell and siphuncle in coiled Mesozoic ammonoids. *Royal Ontario Museum, Life Sciences Contributions 78,* 1–39.

Westermann, G.E.G. 1975: Model for origin, function and fabrication of fluted cephalopod septa. *Paläontologische Zeitschrift 49,* 235–253.

Westermann, G.E.G. 1990: New developments in ecology of Jurassic–Cretaceous ammonoids. *In* Pallini, G., Cecca, F., Cresta, S. & Santantonio, M. (eds.): *Atti II Convengo Internationale Fossili, Evoluzione, Ambiente,* 459–479. Pergola.